



## Article

# Process Line for Waste Heat Recovery in the Production of Stretch Film Based on Compressor Heat Pumps with Environmentally Friendly Refrigerants

Paweł Obstawski, Jacek Słoma, Krzysztof Górnicki \*  and Michał Awtoniuk 

Institute of Mechanical Engineering, Warsaw University of Life Sciences—SGGW, 164 Nowoursynowska Str., 02-787 Warsaw, Poland; pawel\_obstawski@sggw.edu.pl (P.O.); jacek\_sloma@sggw.edu.pl (J.S.); michal\_awtoniuk@sggw.edu.pl (M.A.)

\* Correspondence: krzysztof\_gornicki@sggw.edu.pl

**Abstract:** The production technology for stretch film is highly energy-intensive. Electrical energy is used not only to power individual components of the technological line but also to change the physical state of the raw material (granules) from solid to liquid, which is poured onto the first calender roller. The calender roller must be cooled to solidify the liquid raw material, and the low-temperature heat generated in this process has been treated so far as waste heat and dispersed into the atmosphere. A low-temperature process heat recovery line has been developed, enabling its transformation into high-temperature heat. High-temperature process heat can be utilized in the technological process for the preliminary preparation of raw material when recycled material (regranulate) with highly variable parameters is added to the base material (granules) with strict specifications. The regranulate content can be as high as 80%. The waste heat recovery system is based on two compressor heat pumps powered by eco-friendly refrigerants. This innovative solution facilitates a circular economy, reduces the carbon footprint, and aligns with the European Green Deal.

**Keywords:** technological line; stretch film; recycle; heat pump; greenhouse gas reduction



Academic Editor: George Kosmadakis

Received: 24 November 2024

Revised: 29 December 2024

Accepted: 31 December 2024

Published: 3 January 2025

**Citation:** Obstawski, P.; Słoma, J.; Górnicki, K.; Awtoniuk, M. Process Line for Waste Heat Recovery in the Production of Stretch Film Based on Compressor Heat Pumps with Environmentally Friendly Refrigerants. *Energies* **2025**, *18*, 162. <https://doi.org/10.3390/en18010162>

**Copyright:** © 2025 by the authors. Licensee MDPI, Basel, Switzerland. This article is an open access article distributed under the terms and conditions of the Creative Commons Attribution (CC BY) license (<https://creativecommons.org/licenses/by/4.0/>).

## 1. Introduction

Stretch film is used in various industries, including food, medical, and agricultural sectors, as well as in households. The production of stretch film is most commonly carried out using the cast method, which is highly energy intensive. Moreover, stretch film is produced from polymers whose disposal remains problematic even with waste segregation [1]. The recycling of polymer materials mainly involves so-called energy recovery, which is energy recovery through direct combustion or by producing solid, liquid, or gaseous fuels [2–5]. An example is gasoline production from polyethylene terephthalate (PET) [5]. Research is underway to replace synthetic polymer products with natural, biodegradable, or compostable materials. However, the results are not yet entirely satisfactory and do not allow for the widespread commercialization of such technologies [4,6,7]. Some products have been abandoned or replaced with reusable alternatives, such as returnable bottles, while others have been modified to facilitate recycling [8]. Polymer materials are not easy to recycle. To improve the efficiency of recycling and upcycling, new technologies are being developed, such as thermomechanical processing, chemical recycling (glycolysis and pyrolysis), and biological depolymerization using catalysts, enzymes, and microorganisms [2,3,9,10]. Considering the EU Energy Policy [11], which aims to reduce greenhouse gas emissions,

including CO<sub>2</sub>, and promote a circular economy, attention has been drawn to the potential of reusing polymer waste in stretch film production by adding regranulate to the base material—up to 80% of the raw material volume. The developed technology not only facilitates the realization of a circular economy but also enables the utilization of process heat, which until now was treated as waste heat and dispersed into the environment.

The most commonly used technological process for producing a stretch film by the cast method (Figure 1) involves the following processing steps [12,13]:

- Extrusion—the raw material granules (most commonly low-density polyethylene, LDPE) are heated in a single- or twin-screw extruder to a liquid state (above the melting point). The material is then homogenized and degassed.
- Casting—the molten material is evenly poured onto a rapidly rotating, intensively cooled metal drum, where it solidifies but remains in a visco-liquid state (between the softening point and the glass transition temperature).
- Calendering—the material (now in film form) transitions from a visco-liquid to a visco-elastic state. At this stage, the film is repeatedly passed through calender rollers of varying diameters and rotational speeds, where it is stretched to achieve the desired thickness and mechanical properties.
- Winding—the finished film sheet is wound onto transport or commercial rolls.

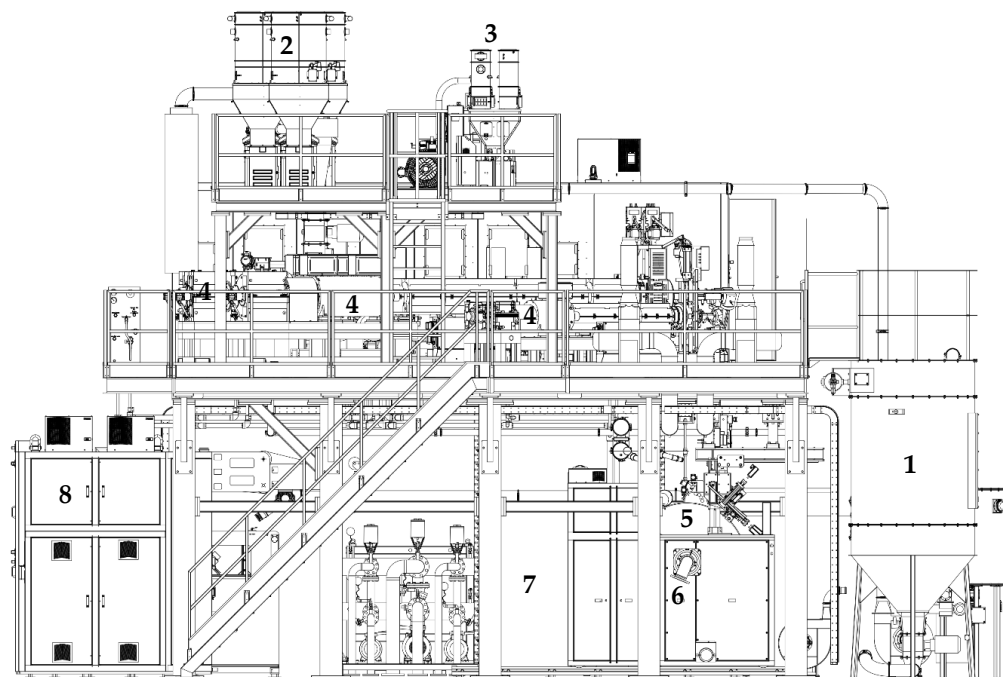


**Figure 1.** Technological line for the production of stretch film using the cast method (1—regranulate tank; 2—extruder buffer tank; 3—extruder buffer tank; 4—extruder; 5—first calender roller; 6—connection of cooling system of the first calender roll; 7—film cooling system; 8—control and monitoring system).

The stable operation of a stretch film production line depends largely on a stable temperature of the first calender roll, onto which liquid regranulate is fed. The roller acts as a cooler, and the heat from the roller cooling process has been treated as waste heat and dissipated in the environment. Increasing the proportion of recycled material fractions in the regranulate, which may originate from various sources, involves standardizing it. Process heat, treated as waste heat, can be used in the technological process of pre-drying and processing recycled material. The use of renewable energy is currently of great interest and importance, considering their implications and contribution to the sustainable development of society and the impact on global warming [14,15].

Heat pumps are widely used as an alternative to other heating devices in commercial buildings [16,17] or industry [18]. They are also increasingly used in waste heat recovery systems. Chen et al. [19] studied absorption heat pumps in recovering waste heat from flue gas; the developed system increased the power output by 1.21 MW compared to the original system in the waste incineration plant. Ghaderi et al. [20] used the heat pump systems to recover ventilation waste heat. The system saves 57% of primary energy. Ma et al. [21] investigated refrigerants in a high-temperature heat pump waste heat recovery system. The traditional refrigerants used in them (hydrofluorocarbons (HFCs)), due to their high GWP (Global Warming Potential) and ODP (Ozone Depletion Potential), are constantly being replaced with environmentally friendly refrigerants, which are still being developed [22–24].

The work aimed to develop a technological line for waste heat recovery in stretch film production, including creating the compressor heat pumps used there. Low-temperature and high-temperature compressor heat pumps will use ecological refrigerants.

## 2. Materials and Methods

Designing a technological line for recovering technological heat involves solving several partial problems.

### 2.1. Selection of the Refrigerant and Compressor

It should be noted that the most critical component of the refrigeration system is the compressor. The fact that the refrigerant meets the technological assumptions does not mean that the possible range of changes in the lower and upper source temperature will coincide with the compressor operating envelope. The selection of the compressor type largely determines its cooling capacity and the possibility of working in tandem, which determines the nominal power of the device. In addition, the compressor design determines the resistance to operating temperatures, resistance to flooding with a liquid agent, and the possibility of changing the oil, affecting the device's service life. Guided by the selection of refrigerants, the types of compressors offered by different manufacturers on the market were analyzed. The main criteria were the possibility of cooperation with the R1234yf agent and the possibility of collaboration with the R1234ze(E) agent, the possibility of working in tandem, which allows the nominal cooling power and heating power of the designed devices to be adjusted to the demand for technological cooling and heat, the possibility of regulating the efficiency of the devices by using frequency converters, the possibility of changing the oil, and resistance to flooding with a liquid agent.

The limitation of the choice of the refrigerant is the refrigerant phase-out schedule specified in the EU directive (Regulation of the European Parliament and the Council (EC) No. 517/2014 (of 16 April 2014) on fluorinated greenhouse gases) [25], according to which it is prohibited to introduce to the market refrigeration equipment powered by refrigerants with a GWP coefficient  $> 150$  [26,27].

The low-temperature compressor heat pump is based on two parallel semi-hermetic piston compressors manufactured by Bitzer (Sindelfingen, Germany). From the available series, the compressor with the catalogue number 8FE-60Y was selected, and the operating envelope for the R1234yf agent (critical point parameters: 80 °C, 25 bar) is shown in Figure 2 [13]. The operating envelope shows that the range of the refrigerant saturation temperature is from  $-20$  °C to 25 °C, while the refrigerant condensation temperature is limited to the range of 20 °C to 80 °C. Due to the technical parameters of the first calendar roll—coolant temperature 15 °C, it was assumed that the design (nominal) saturation temperature of the refrigerant of the low-temperature heat pump would be 5 °C. This design assumption results from the technical parameters of the plate heat exchanger acting as an evaporator. Considering the intensity of the heat exchange process at the design stage,

it is assumed that the gradient between the saturation temperature of the refrigerant and the lower source temperature is 10 K. For this reason, considering the work envelope for the high-temperature compressor of the subcritical heat pump supplied with 1234 ze(E) refrigerant (critical point parameters: 100 °C, 30 bar), it was assumed that the nominal operating point of the low-temperature heat pump would be determined for the saturation temperature of the refrigerant of 5 °C and the condensation temperature of the refrigerant of 35 °C. In the design studies, it was assumed that the superheating of the refrigerant would be 10 K, and the subcooling would be 5 K (Figure 3).

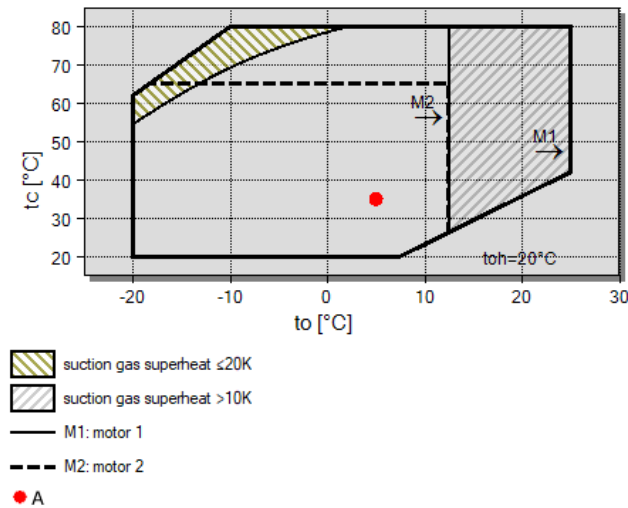


Figure 2. Operating envelope of the 8FE-60Y compressor.

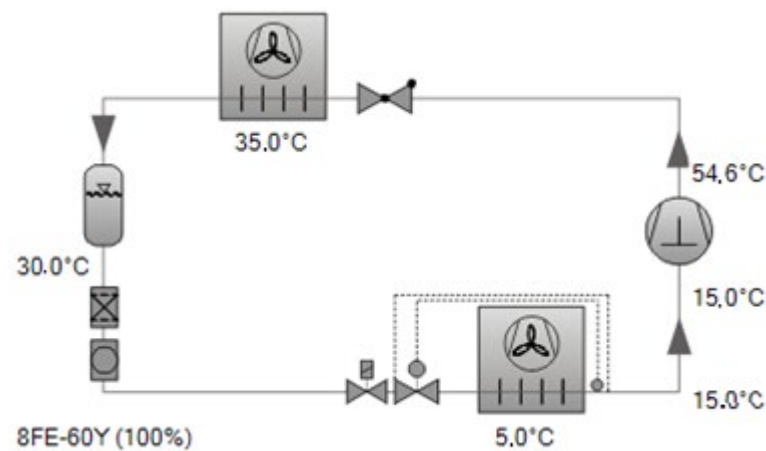


Figure 3. Operating parameters of a low-temperature compressor heat pump.

Figure 4 shows the thermodynamic cycle of heat pumps in the T-s diagram. The cycle takes into account the superheating and subcooling of refrigerant. It consists of the following stages: 1–2 adiabatic compression, 2–3 isobaric cooling of superheated steam, isobaric-isothermal condensation and cooling of the refrigerant in the liquid phase, 3–4 isenthalpic expansion, 4–1 isobaric-isothermal evaporation and isobaric heating of superheated steam.

The high-temperature compressor heat pump is based on two parallel (tandem) connected semi-hermetic piston compressors manufactured by Bitzer. From the available series, a compressor with the catalogue number 6FEH-50Y was selected; the operating envelope for the R1234ze(E) agent is shown in Figure 5.

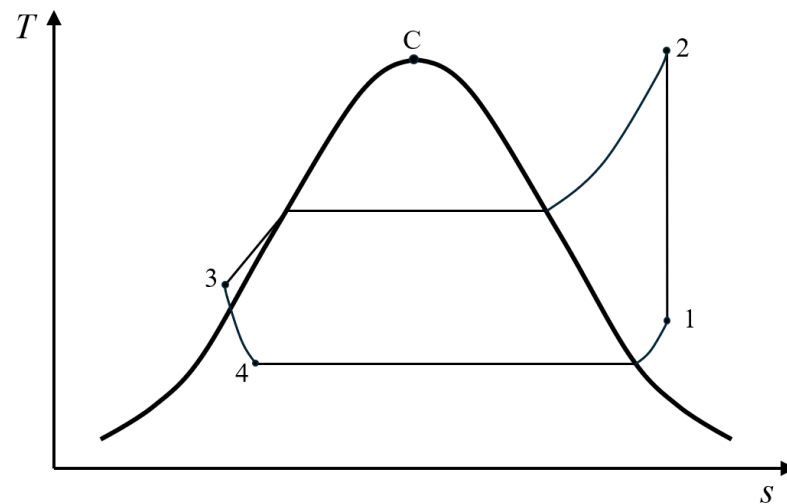


Figure 4. The thermodynamic cycle (with the superheating and the subcooling) of heat pumps in T-s.

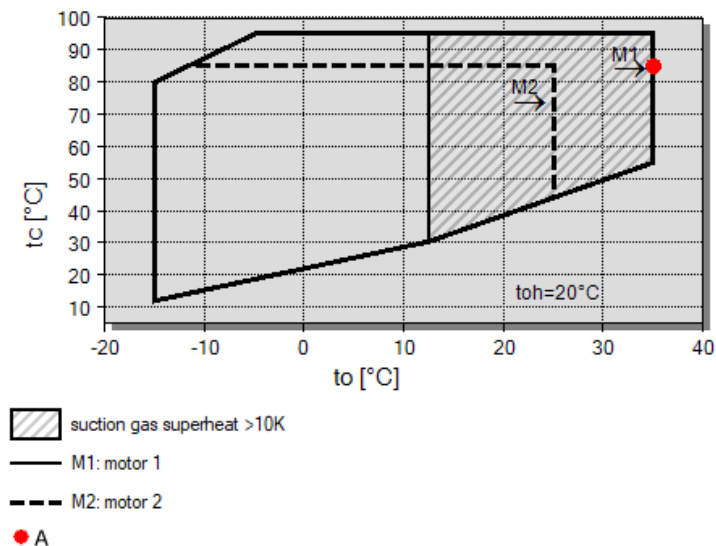
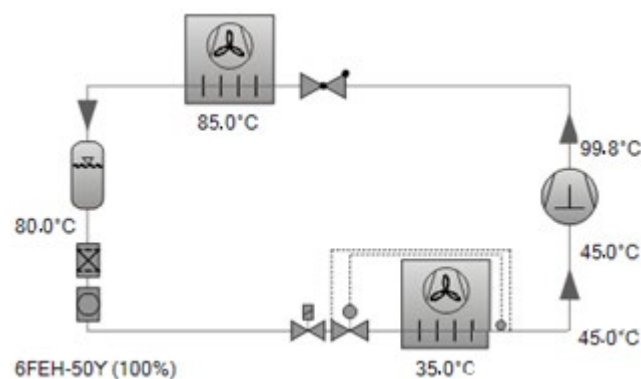


Figure 5. Operating envelope of the 6FEH-50Y compressor.

The operating envelope shows that the range of the refrigerant saturation temperature is from  $-15\text{ }^{\circ}\text{C}$  to  $35\text{ }^{\circ}\text{C}$ , while the condensation temperature of the refrigerant is limited to the range of  $10$  to  $95\text{ }^{\circ}\text{C}$ . Due to the technical parameters of the low-temperature heat pump operation, or more precisely, the range of possible upper heat source temperatures ( $25$ – $50\text{ }^{\circ}\text{C}$ ), by the compressor operating envelope, it was assumed that the range of the refrigerant saturation temperatures is from  $16$  to  $30\text{ }^{\circ}\text{C}$ . This design assumption results from the technical parameters of the plate heat exchanger acting as an evaporator. Considering the intensity of the heat exchange process at the design stage, it is assumed that the gradient between the saturation temperature of the refrigerant and the lower source temperature is  $10\text{ K}$ . For this reason, considering the work envelope for the high-temperature compressor of the subcritical heat pump supplied with  $1234\text{ ze(E)}$  agent, it was assumed that the nominal operating point of the low-temperature heat pump will be determined for the saturation temperature of the refrigerant of  $35\text{ }^{\circ}\text{C}$  and the condensation temperature of the refrigerant of  $85\text{ }^{\circ}\text{C}$ . Considering the technological process's requirements, the upper source temperature range was assumed to be  $75$ – $85\text{ }^{\circ}\text{C}$ . The design studies assumed that the refrigerant superheating has been  $10\text{ K}$  and subcooling  $5\text{ K}$  (Figure 6).



**Figure 6.** Operating parameters of a high-temperature compressor heat pump.

## 2.2. Cooling System

As mentioned, it was assumed that the refrigerant superheat was 10 K and subcooling was 5 K. The calculations were performed using the Bitzer software [28]. The refrigerant mass flow rate  $\dot{m}$  (in kg/s), knowing the compressor volumetric efficiency  $V$  (in  $\text{m}^3/\text{s}$ ), and the specific steam volume  $v$  (in  $\text{m}^3/\text{kg}$ ) at the suction nozzle (for the assumed temperatures from the refrigerant p-h diagram) were calculated from the relationship (1)

$$\dot{m} = \frac{V}{v} \quad (1)$$

Thermodynamic calculations of the refrigeration system were performed in the Matlab & Simulink Thermolib Basic package. The heating power, cooling power, compressor power, COP coefficient, heat transfer coefficient of the evaporator and condenser (necessary for complete evaporation and condensation of the refrigerant) and the flow of the working medium (being the heat carrier; temperature gradients were assumed on the primary side of the evaporator 3 K and the secondary side of the condenser 5 K) were determined.

The diameter (inner diameter of the pipe) of the discharge line was estimated assuming that the refrigerant flow velocity would be variable in the range of 8–20 m/s, the high-pressure liquid line would be in the range of 0.5–1.5 m/s, the low-pressure liquid line would be in the range of 0.4–0.5 m/s, and the refrigerant flow velocity in the suction line would be greater than eight m/s. The diameters  $d$  (in m) of the individual sections of the refrigeration system were calculated from the relationship (2).

$$d = \sqrt{\frac{4 \cdot V}{\pi \cdot v}} \quad (2)$$

## 2.3. Compressor Heat Pump Construction

The low-temperature and high-temperature compressor heat pump construction was developed using SolidWorks 2021 software.

## 3. Results

### 3.1. Description of a Process Line for Waste Heat Recovery

To maintain the high quality of the resulting film at such a high production rate, it is necessary to maintain a constant temperature of the first roll—the calender [29]. The need to cool this roller and the large amount of waste heat generated here prompted researchers from the Department of Fundamentals of Engineering at the Warsaw University of Life Sciences to design a line to recover this heat and use it in the technological process of stretch film production. The technological line consists of two hydraulic systems separated by a

plate heat exchanger (Figure 7). Heat pump evaporators or fan coolers supply the primary side of the exchanger as the source of process cooling. The load for the secondary side of the heat exchanger (plate exchanger) is the hydraulic installation enabling the reception of the mentioned technological heat from the first calender cylinder.

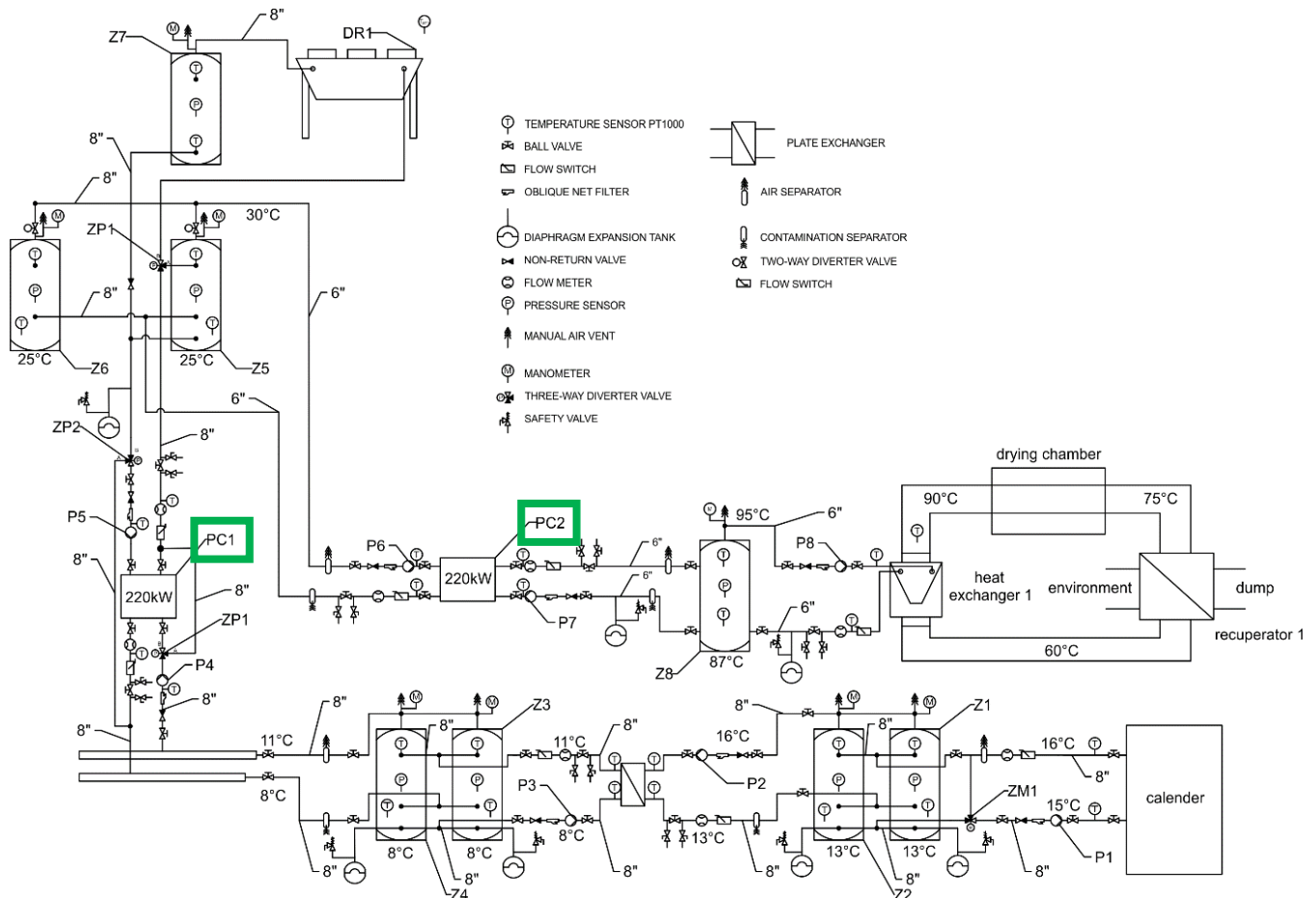


**Figure 7.** Hydraulic system diagram for process heat recovery.

The even surface temperature of the rotating cylinder is ensured by the appropriate water flow (inlet and outlet temperatures: 15 and 16 °C, respectively) of about 150 m<sup>3</sup>/h. During film production, about 176 kW of waste heat (low temperature) is generated, which would be dispersed in the atmospheric air. The innovation of the process is using this heat for drying regranulate thanks to the increase in the temperature level of waste heat. The increase in the temperature level of low-temperature waste heat is achieved using a specially designed heat recovery system based on two compressor heat pumps powered by ecological refrigerants, i.e., agents with low ODP and GWP coefficients. The main technological problem is ensuring a stable and constant inlet water (coolant) temperature in the cylinder. Therefore, two parallel-connected buffer tanks (Z1 and Z2) with a volume of 2000 dm<sup>3</sup> each (simultaneously increasing the water charge in the installation) were used as cold storage. The water pump P1, with smooth regulation of its capacity, enables modification of the water inlet temperature to the calender (three-way mixing valve ZM1 with smooth regulation). The essential source of cooling (the first stage of technological heat recovery) is the compressor heat pump PC1 designed by employees of the Department of Fundamentals of Engineering and Energy at the Institute of Mechanical Engineering at the Warsaw University of Life Sciences (nominal power according to the PNEN 14511 standard (temperatures of the lower and upper heat source are 10 and 35 °C, respectively) is 220 kW), the lower heat source of which is the energy necessary to cover the cooling demand of

the calender. PC1 uses semi-hermetic piston compressors, whereby the adjustment of its cooling power (to the current cooling demand of the calender) is achieved thanks to the inverter (regulation of the compressor supply voltage frequency: 30–50 Hz) regulating the compressor capacity. The PC1 evaporator is hydraulically coupled to buffer tanks Z3 and Z4 (2000 dm<sup>3</sup> each) and thanks to the plate heat exchanger (separation between glycol and water on the primary and secondary sides of the heat exchanger, respectively) with Z1 and Z2. Water pump P2 (with smooth regulation of its capacity) causes water flow between the secondary side of the exchanger and Z1 and Z2, while pump P3 (with smooth regulation of its capacity—ensuring a constant temperature gradient: 3K) causes glycol flow between buffer tanks Z3 and Z4 and the primary side of the plate heat exchanger. The pump P4 (with smooth regulation of its capacity: maintaining a constant difference between the inlet and outlet temperature of glycol to the evaporator 3 K, ensuring high efficiency of PC1) causes glycol flow between buffer tanks Z3 and Z4 and the evaporator of PC1. The condenser of PC1, depending on the operating mode (dependent on the current heat demand of the high-temperature technological process of preliminary preparation of regranulate), discharges heat to buffer tanks Z5 and Z6 (2000 dm<sup>3</sup>) or fan cooler DR1. The PC1 operating mode is set by changing the position of three-way switching valves ZP1 and ZP2. The first mode of operation of the heat pump PC1 (valves PZ1 and ZP2 in position B) consists of supplying heat to buffer tanks Z5 and Z6 (heat load for the evaporator of the high-temperature heat pump PC2). However, if PC2 is not started or when the temperature in Z5 and Z6 has reached the set point, the following two modes of operation are possible. When the ambient temperature is higher than 3 °C, the medium-temperature heat is dispersed in the environment using the DR1 fan cooler; the buffer tank Z7 increases the glycol charge in the installation (it has a beneficial effect on the length of the heat pump operation cycle). However, when the glycol temperature in Z5 and Z6 reaches the set point, and the ambient temperature is lower than 3 °C, then the ZP1 and ZP2 valves are in position A, and the glycol flow between Z3 and Z4 and DR1 is forced using the P4 pump. This solution allows for significant savings in the electrical energy required to drive PC1 (in this mode, it is switched off). The high-temperature compressor heat pump PC2 enables the generation of high-temperature technological heat. The lower source of PC2 is Z5 and Z6, and the heat load of its condenser is the buffer tank Z8 (high-temperature heat source for the V-type heat exchanger). The heat exchanger is a source of heat used in the preliminary drying process of the regranulate. Details about the technological line for waste heat recovery can be found in our earlier publication [30].

Based on the technical data from the Project Leader, it was estimated that the demand for technological cooling of the first calender roll would be 176 kW. This value was the basis for the design calculations of individual components of the technological heat recovery line. The demand for technological cooling of the first calender roll with a power of 176 kW and a temperature of 15 °C is the design value of the cooling power of a low-temperature, single-stage heat pump. The heating power and electrical energy required to drive the compressor will be variable and dependent on other operating parameters, including the necessary temperature of the upper source of the first stage of the heat recovery system and the volumetric efficiency of the compressor, which, by the design assumptions, can be regulated using frequency converters.

Analyzing the technical documentation of compressors available on the market in terms of selected refrigerants and the value of the nominal calculated cooling capacity of the first calender roll, it was decided that the most advantageous solution from the technological and economic point of view (taking into account investment and operating costs) would be to design a refrigeration device based on two semi-hermetic Bitzer piston compressors. The use of such a solution meets all the design assumptions. It allows for



performing service activities that affect the length of the compressor's life cycle, including replacing operating fluids (oil) and oil filters. It is also possible to regenerate the compressor if necessary.

### 3.2. Low-Temperature Subcritical Compressor Heat Pump

Knowing the compressor volumetric capacity of 221 m<sup>3</sup>/h (and for the assumed temperatures, the value of the specific volume of steam at the suction nozzle (p-h diagram of the R1234yf refrigerant using Equation (1), the mass flow of the refrigerant was calculated (Table 1).

**Table 1.** Refrigerant mass flow  $\dot{m}$  (in g/s) for assumed design refrigerant saturation and condensation temperatures.

$t_{or}$ , °C	10	8	6	4	2	0	−2	−4	−6	−8	−10	−12	−14	
$t_c$ , °C	25	1247.2	1157.8	1073.9	995.6	921.9	852.8	788.1	727.2	670.3	616.7	566.4	519.4	475.3
	30	1230.8	1142.2	1059.2	981.1	908.1	839.4	775.3	715.0	658.3	605.0	555.3	508.3	464.7
	35	1213.3	1125.3	1043.1	965.8	893.3	825.3	761.4	701.7	645.3	592.5	543.1	496.7	453.1

Based on the mass flow of the refrigerant for the assumed design values of the refrigerant saturation and condensation temperature, thermodynamic calculations of the refrigeration system were performed in the Matlab&Simulink Thermolib package to determine the heating power, cooling power and compressor power.

### 3.3. Simulation Studies of the Refrigeration System in the Matlab Simulink Thermolib Package

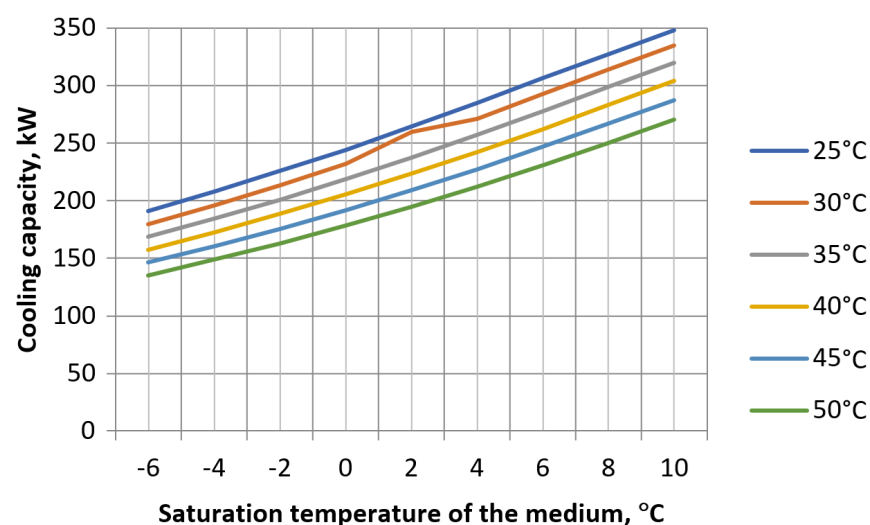
The simulation studies were aimed at determining the following for the assumed device operating envelope: heating power, cooling power, electric energy consumed by the compressor, COP coefficient, heat transfer rate (in W/K) of the evaporator and condenser necessary for complete evaporation and condensation of the refrigerant and determining the required flow of the working medium being the heat carrier for the assumed design work gradients on the primary side of the 3 K evaporator and the secondary side of the 5 K condenser. The simulation studies began with the design of the refrigeration system according to the adopted single-stage system. At key points of the designed refrigeration system, the mass flow, temperature, pressure and, based on humidity, the state of matter of the refrigerant were examined.

From the design point of view, it was essential to determine the value of the total heat loss coefficient of the evaporator and condenser as a function of the mass flow of the medium on the primary side in the case of the evaporator and on the secondary side in the case of the condenser. In the case of the evaporator, the medium on the primary side was water; in the case of the condenser, the medium on the secondary side was a 40% ethylene glycol solution with a solidification temperature of −35 °C. From the operational point of view, it is essential to determine the mass flow on the primary side of the evaporator and the secondary side of the evaporator at which, for the assumed design temperature difference of the medium (evaporator 3 K, condenser 5 K), the medium will change its state of aggregation—in the case of the evaporator to gas and in the case of the condenser to liquid.

For this reason, PI controllers were designed to regulate the flow on the evaporator's primary and the condenser's secondary sides, the input signal of which was the control deviation between the set temperature gradient and the measured value. Simulation studies were started by finding the most unfavorable operating point of the compressor subcritical heat pump; i.e., finding such an operating point defined by the operating envelope at which the heating power and cooling power have the highest values. By determining for this operating point the value of the total heat loss coefficient of the exchanger for which the

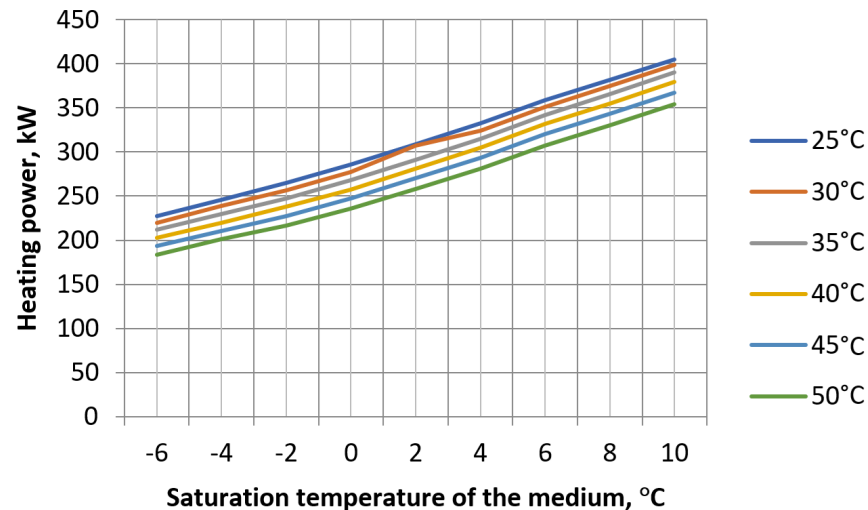
refrigerant will change its state of matter in the case of the evaporator to gas and in the case of the condenser to liquid, for the assumed temperature gradient, it is possible to calculate the required minimum flow number of the evaporator and condenser. For all other operating points located in the device's operating envelope, the selected heat exchange surface of the evaporator and condenser will be greater than the minimum required, as a result of which the refrigerant will continuously be evaporated in the case of the evaporator and always condensed in the case of the condenser. In the case of the 1234yf agent, the most unfavorable operating point (operating point characterized by the highest cooling power and heating power) turned out to be the operating point for the highest saturation temperature of the refrigerant and the lowest condensation temperature. For the agent to change its state of matter to gas, the value of the total heat transfer coefficient of the evaporator was 132,000 W/K, while in the case of the condenser, the value of this coefficient was 84,000 W/K.

Figure 8 shows the cooling capacity of a low-temperature heat pump for a wide range of condensation (from 25 to 50 °C) and saturation (from −6 to 10 °C) temperatures. It can be seen that the cooling capacity increases with increasing saturation temperatures and decreasing condensation temperatures. The available cooling power corresponds to the technological cold for cooling the first calender roll. The nominal operating point is 4 °C and 35 °C (saturation and condensation temperature, respectively). The deviation of the parameters visible in Figures 8 and 9 (2 °C and 30 °C) results from the isentropic efficiency of the compressor (the manufacturer's catalogue data were used in the calculations).



**Figure 8.** Cooling capacity graph of a low-temperature heat pump with 100% control of both compressors for refrigerant condensing temperatures 25–50 °C.

The dependence of heating power on the refrigerant's saturation temperature is presented similarly (Figure 9). The device generates the highest heating power value of 405 kW for the refrigerant's highest design saturation temperature (10 °C) and the lowest condensation temperature (25 °C). For this operating point, the power of both compressors is 39 kW. In the case of an increase in the condensation temperature from 25 °C to 50 °C at a constant saturation temperature of the refrigerant of 10 °C, the heating power received from the condenser will decrease from 405 to 354 kW, and the compressor power will increase to 87.2 kW. The lowest value of heating power is obtained for the saturation temperature of the refrigerant of −6 °C and its condensation temperature of 50 °C. The heating power value for this operating point is 183.8 kW with a demand for compressor power of 38.8 kW.



**Figure 9.** Heating power graph of a low-temperature heat pump with 100% control of both compressors for refrigerant condensing temperatures 25–50 °C.

A specific trend can be observed when analyzing the power variation in compressors controlled at 100% as a function of the refrigerant saturation temperature. In the entire range of the refrigerant saturation temperature for the lowest value of the refrigerant saturation temperature, the total power of both compressors operating at maximum volumetric efficiency is practically constant at 40 kW. The higher the refrigerant condensation temperature, the higher the electricity consumption, and the higher the refrigerant saturation temperature (Figure 10). At the highest tested condensation (50 °C) and saturation (10 °C) temperatures of the refrigerant, the demand for compressor power is almost 90 kW.

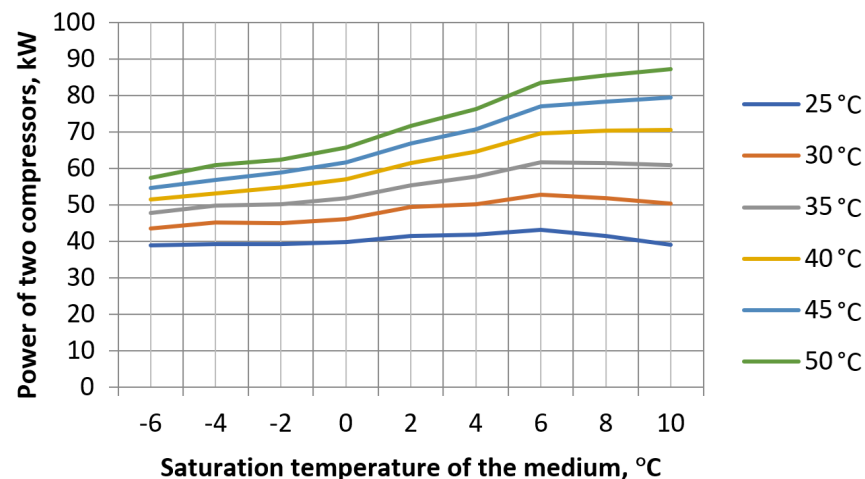


**Figure 10.** Power diagram of two compressors of a low-temperature heat pump at 100% control for refrigerant condensing temperatures 25–50 °C.

As a result (Figure 11), the most significant COP variability over the entire range of refrigerant saturation temperature is achieved by the designed device at the lowest condensation temperature constant over time, which is 25 °C. For a refrigerant saturation temperature of 10 °C and a condensation temperature of 25 °C, the maximum COP value of 10.37 is achieved. The minor COP variability over the entire range of refrigerant saturation temperature occurs for the highest condensation temperature of 50 °C: the average 3.8. For the nominal operating point (4 °C and 35 °C, saturation temperature and condensation temperature, respectively), the COP is 5.5.

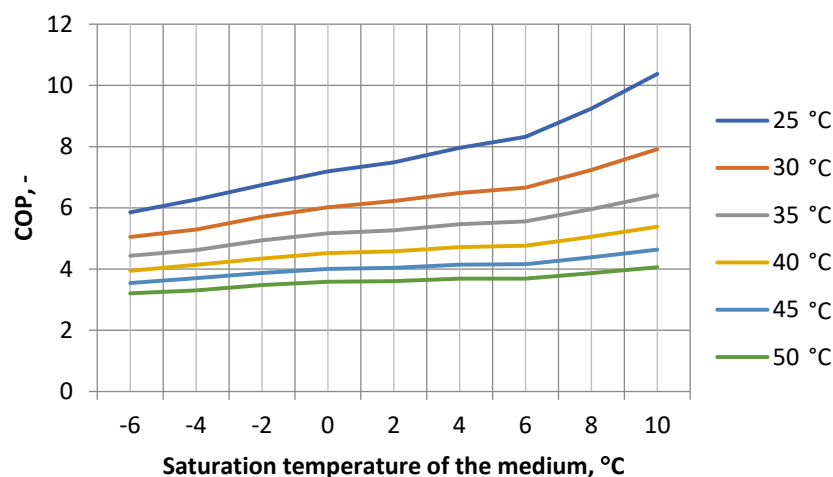


**Figure 11.** The COP value of the low-temperature heat pump with 100% control of both compressors for refrigerant condensing temperatures 25–50 °C.

The COP value is determined by the temperature of the lower and upper heat sources, which determines the saturation and condensation temperature of the refrigerant. As was mentioned, in the case of a low-temperature heat pump, the COP is determined by the required temperature of the technological medium cooling the first calender roll. The nominal temperature of the medium is 16 °C, and the heat exchanger was designed for the difference between the temperature of the medium and the refrigerant saturation temperature of 10 K. Therefore, the nominal saturation temperature is 6 °C. The temperature of the upper heat source depends on the required temperature of the technological process: whether the heat is dissipated in the atmosphere or used for drying. The computer simulations shown in Figures 8–11 concern a wide range of temperatures (condensation: from 25 to 50 °C and saturation from –6 to 10 °C) for which COP values were obtained (even COP > 10).

Analyzing the quality of regulation obtained using the designed PI controllers, it is visible that in the case of the evaporator, the maximum regulation deviation is 0.35 °C. The smallest is close to 0 (Figure 12). In the condenser case, the maximum regulation deviation is 0.35 °C, and the minimum equals 0 (Figure 13). The reason for the deviation of the parameters in Figures 12 and 13 results from the mass flow of the working medium. The temperature delta was not achieved exactly as 3.0 and 5.0 (3.12, 3.15, 3.25, 3.37 and 4.83, 5.11, 5.37, respectively).

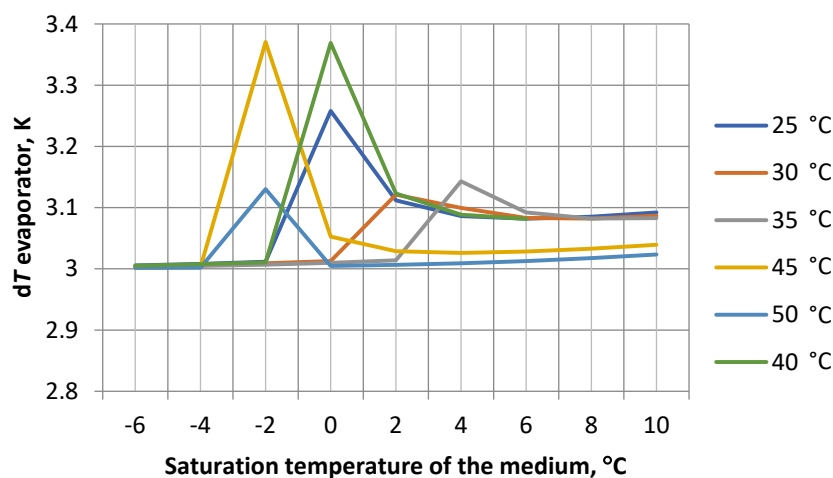


**Figure 12.** Quality of dT regulation of the working medium flowing through the evaporator of a low-temperature heat pump with 100% control of both compressors for refrigerant condensing temperatures 25–50 °C.

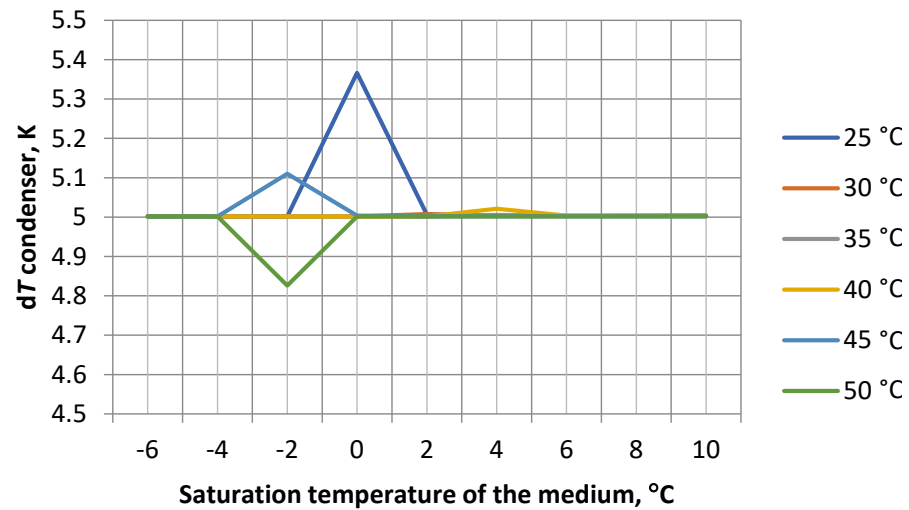


**Figure 13.** Quality of dT regulation of the working medium flowing through the condenser of a low-temperature heat pump with 100% control of both compressors for refrigerant condensing temperatures 25–50 °C.

The simulation studies allowed the calculation of the required flow of the working medium on the evaporator's primary and the condenser's secondary sides. For both the evaporator and the condenser, the required flow of the medium increases linearly for a constant saturation temperature of the refrigerant and an increase in the lower source temperature. In the case of the evaporator, the most enormous volumetric flow is 2217.5 dm<sup>3</sup>/min, and in the case of the condenser, the maximum flow value is 1582.1 dm<sup>3</sup>/min. The calculated values of the mass flow through the evaporator and condenser allowed the selection of circulation pumps, forcing the working medium's flow through the evaporator's primary and the condenser's secondary sides (Figures 14 and 15).

The fact that the piston compressors can regulate volumetric efficiency in the range of 30–50 Hz allows the device's efficiency to be adjusted to the current demand for technological cooling.

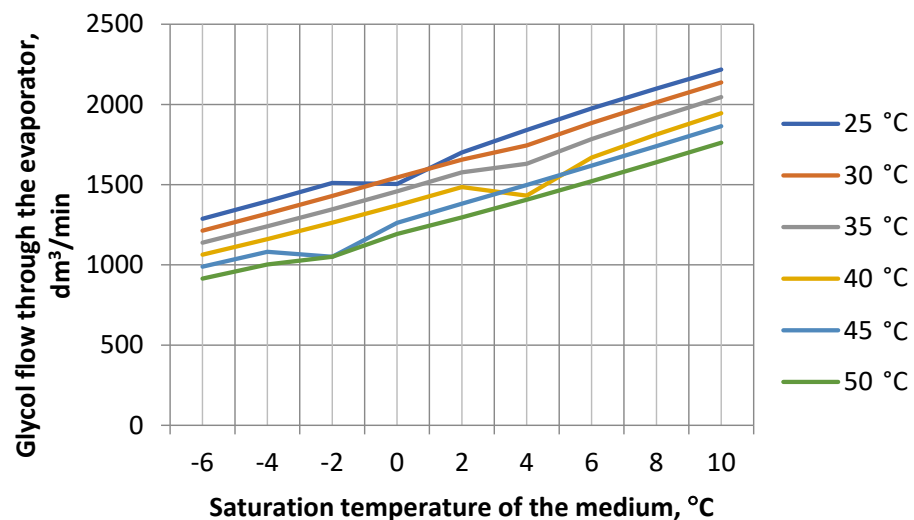


**Figure 14.** Volume flow of the working medium through the evaporator of a low-temperature heat pump with 100% control of both compressors for refrigerant condensing temperatures 25–50 °C.

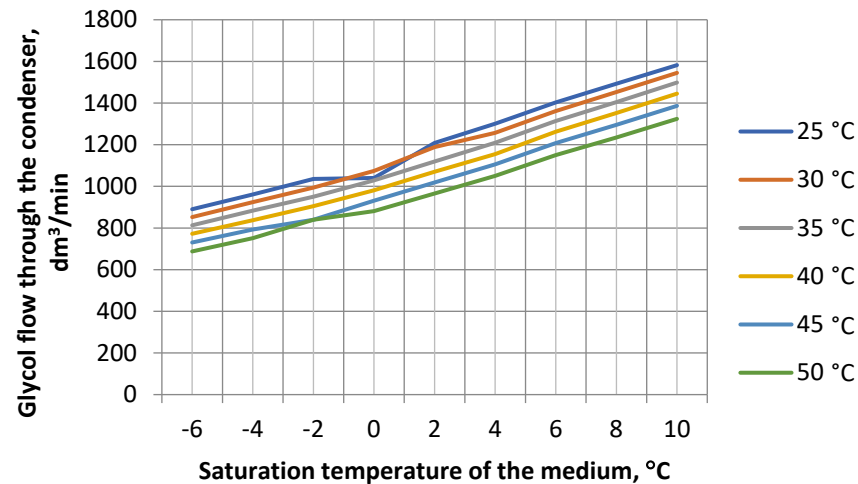


**Figure 15.** Volume flow of the working medium through the condenser of a low-temperature heat pump with 100% control of both compressors for refrigerant condensing temperatures 25–50 °C.

### 3.4. Selection of Structural Elements and Dimensioning of Pipes for the Refrigeration System of a Low-Temperature Compressor Heat Pump

Based on the simulation studies, a refrigeration system for a low-temperature subcritical compressor heat pump was developed (Figure 16).

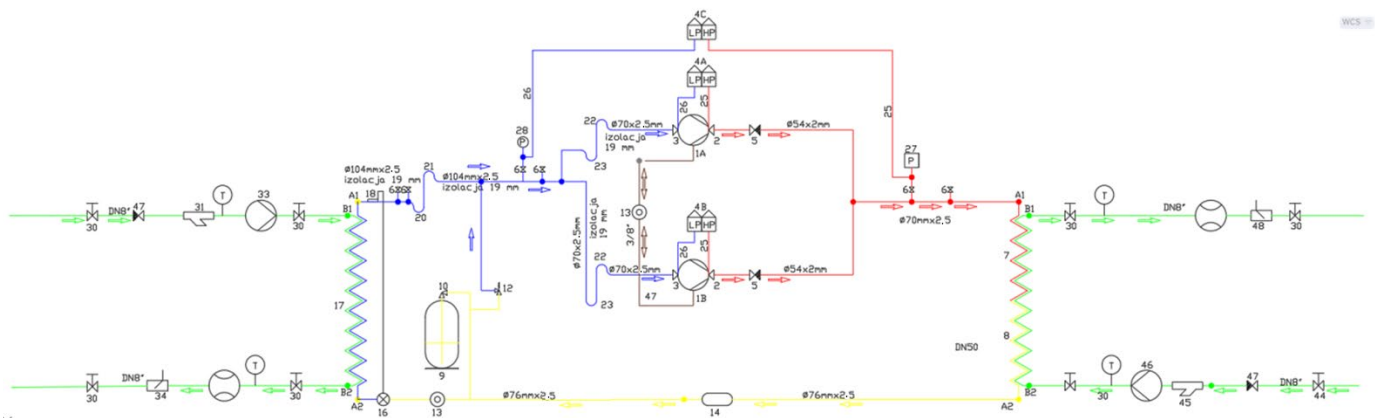


**Figure 16.** Refrigeration system of a low-temperature compressor, subcritical heat pump.

The discharge line is marked in red, the suction line is in liquid, and the liquid line is in yellow. The oil line is marked in brown. The refrigeration system is based on two semi-hermetic piston compressors connected in parallel (tandem). In the event of the need to perform service activities, a rota-lock valve is installed on each compressor's suction and discharge nozzles. Since the system can be operated depending on the demand for technological cooling with one or two compressors switched on, a non-return valve is installed on the discharge nozzle of each compressor. A high and low-pressure transducer is installed in the discharge and suction lines, respectively, providing information on the current value of the refrigerant pressure using an analogue voltage signal in the range of 0–10 V DC. High and low-pressure analogue transducers also constitute the first level of protection of the refrigeration system against too-high and too-low refrigerant pressure. In addition, the second and third levels of security in mechanical pressure switches were used to protect against too-low and too-high pressures. The second level protects individual compressors, while the third level protects both. Plate heat exchangers were used as the evaporator and condenser. A filter drier was installed in the liquid line to protect the motor expansion valve, and a sight glass was used to assess the refrigerant's state. Due to the possibility of operating one or two compressors and due to the possibility of

regulating their capacity, a liquid refrigerant reservoir was installed in the fluid line. It is a refrigerant storage facility that adjusts the appropriate amount of refrigerant depending on the temperature of the lower and upper source and the volumetric capacity of the compressors. A safety valve was used to protect the system against high pressure. The safety valve was connected in parallel to the evaporator by connecting the inlet nozzle of the valve with a pipe to the high-pressure liquid line and the outlet nozzle with a pipe to the suction line. It should be noted that it was connected between two siphons that also function as a liquid separator. This solution protects the compressor from being flooded with a liquid agent in the event of low superheating of the agent and a change in the evaporator's cooling capacity. The compressor oil pans were connected with an oil line, in which a sight glass was installed. The oil line is designed to equalize the oil level in the oil pans if only one compressor is switched on. This solution ensures correct oil distribution in the device's refrigeration system. To protect the suction line from the condensation of water vapor contained in the air and, as a result, from frosting, a 19 mm thick rubber insulation was used. The diameters of individual sections of the refrigeration system were selected based on Equation (2).

The design problem related to the selection of diameters is that depending on the temperature of the lower and upper source of the specified work envelope, the volume flow of the refrigerant is variable due to the change in the density of the refrigerant. The diameter of the discharge line was estimated assuming that the refrigerant flow rate would be variable within the range of 8–20 m/s, the high-pressure liquid line within the range of 0.5–1.5 m/s, the low-pressure liquid line within the range of 0.4–0.5 m/s, and the refrigerant flow rate in the suction line would be greater than 8 m/s. The selected diameters of the individual sections of the refrigeration system were marked on the diagram (Figure 16).

SolidWorks software was used to model the low-temperature compressor heat pump. The construction is based on a steel frame made of rectangular steel bars. The frame is placed on legs made of round steel bars (Figure 17).

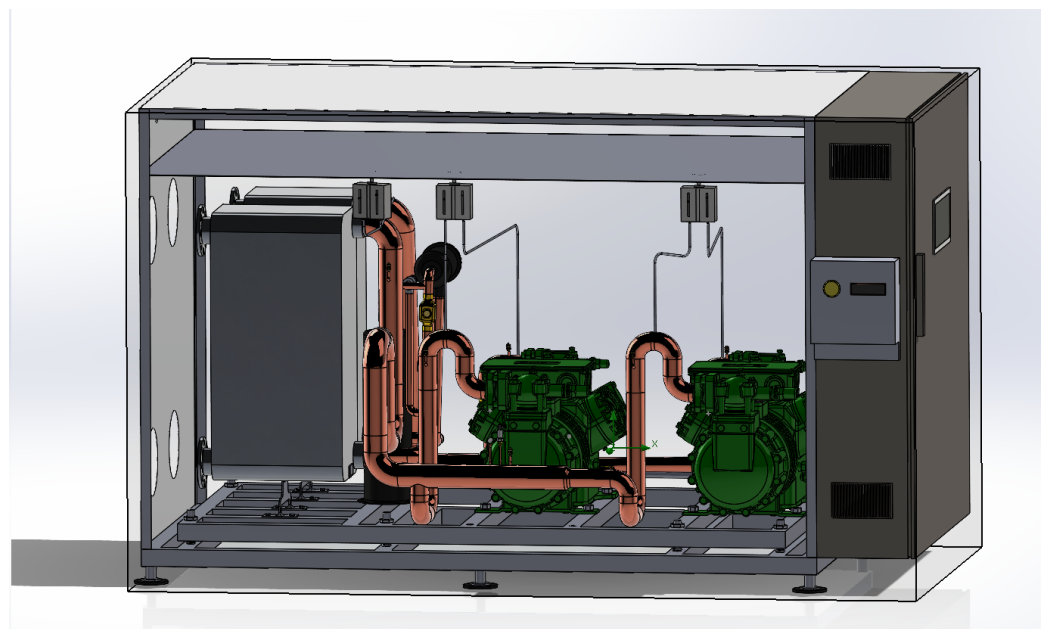


**Figure 17.** Low-temperature compressor heat pump, side view.

To reduce vibrations caused by the compressors, the cooling system is placed on springs where guides are mounted. The designed device is 2270 mm long, 1127 mm wide and 1350 mm high. The actual dimensions of the device may differ from those of the design because the width and length of the device primarily result from the technology used

by the manufacturer to make bends, siphons, and counter-siphons. In the case of using ready-made bends or elbows, regardless of the connection technology, the actual dimension should be consistent with the design. In the case of using pipe bending technology, the dimension of the device will be larger than the design one. The front of the device is the control cabinet, which contains the electrical installation with protections, the controller and the operator panel.

### 3.5. High-Temperature Heat Pump

An analogous procedure was followed for the high-temperature subcritical compressor heat pump.

Knowing the volumetric capacity of the compressor of 156 m<sup>3</sup>/h, and for the assumed temperatures, the value of the specific volume of steam at the suction nozzle (p-h diagram of the R1234yf refrigerant), the mass flow of the refrigerant was calculated using Equation (1) (Table 2).

**Table 2.** Refrigerant mass flow  $\dot{m}$  (in g/s) for assumed design refrigerant saturation and condensation temperatures.

$t_{or}, ^\circ\text{C}$		30	28	26	24	22	20	18	16
$t_c, ^\circ\text{C}$	75	1033.1	961.7	894.4	830.8	771.0	715.0	661.9	612.2
	80	1005.0	936.4	871.7	810.3	752.5	697.8	646.1	597.5
	85	969.4	905.3	843.9	785.8	730.3	677.8	628.1	580.8

Based on the mass flow of the refrigerant for the assumed design values of the refrigerant saturation and condensation temperature, similar to the low-temperature heat pump, thermodynamic calculations of the refrigeration system were performed in the Matlab & Simulink Thermolib Basic package to determine, among others, heating power, cooling power, compressor power, and COP coefficient. Figures 18–25 show the operating parameters of both compressors' high-temperature heat pump at 100% control (supply voltage frequency 50 Hz). Figure 18 shows a graph of the cooling power of the designed low-temperature heat pump for the saturation temperature of the refrigerant in the range of 1–30 °C, which corresponds to the lower source temperature in the range of 26–40 °C, for refrigerant condensation temperatures in the range of 75–85 °C. The graph shows that the highest value of cooling power necessary to evaporate the refrigerant (the most unfavorable operating point of the device from the design point) occurs for the highest saturation temperature of the refrigerant of 30 °C and the lowest condensation temperature of the refrigerant of 75 °C, and the value of cooling power necessary to evaporate the refrigerant is 218 kW. As can be seen from the graph, the cooling power of the designed heat pump, even with 100% control of both compressors, can be adjusted to the current demand for technological cooling by regulating the value of the condensation temperature of the refrigerant. For example, at a constant saturation temperature of 30 °C, increasing the value of the condensation temperature of the refrigerant from 75 °C to 85 °C, the cooling power decreases from 218 to 190.4 kW. The lowest value of cooling power is obtained for the refrigerant condensation temperature of 85 °C at its saturation temperature of 16 °C. The cooling power value for this operating point is 130.2 kW.



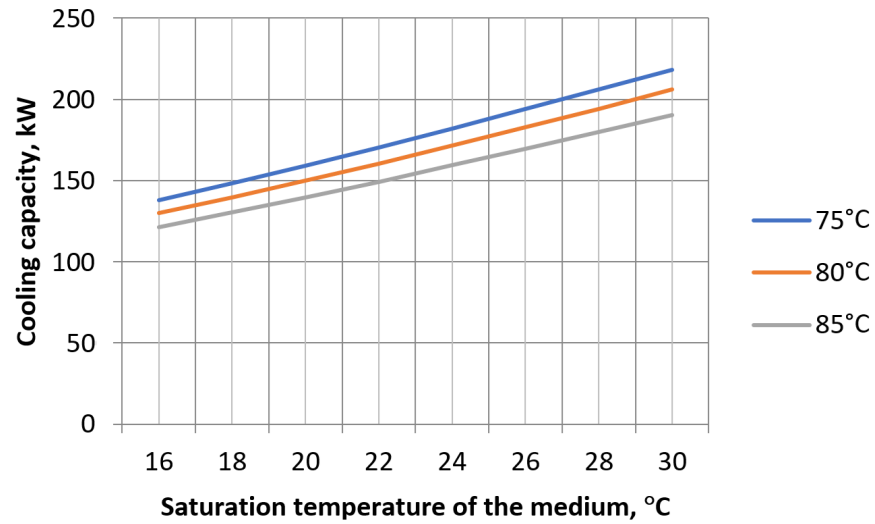


Figure 18. Cooling capacity graph of a high-temperature heat pump with 100% control of both compressors for refrigerant condensing temperatures 75–85 °C.

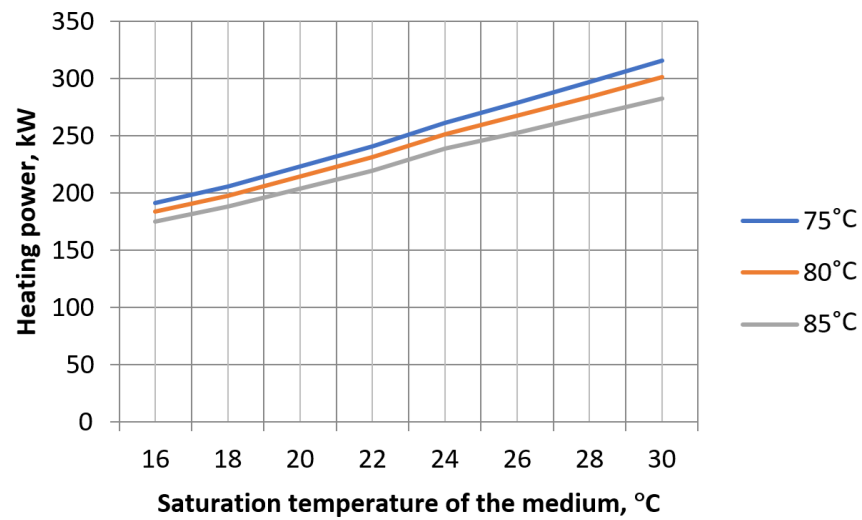


Figure 19. Heating power graph of a high-temperature heat pump with 100% control of both compressors for refrigerant condensing temperatures 75–85 °C.

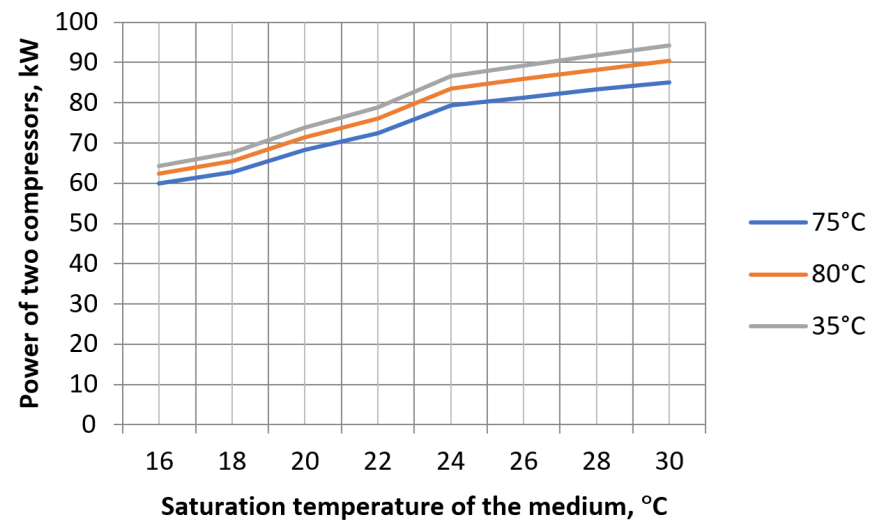


Figure 20. Power diagram of two compressors of a high-temperature heat pump at 100% control for refrigerant condensing temperatures 75–85 °C.

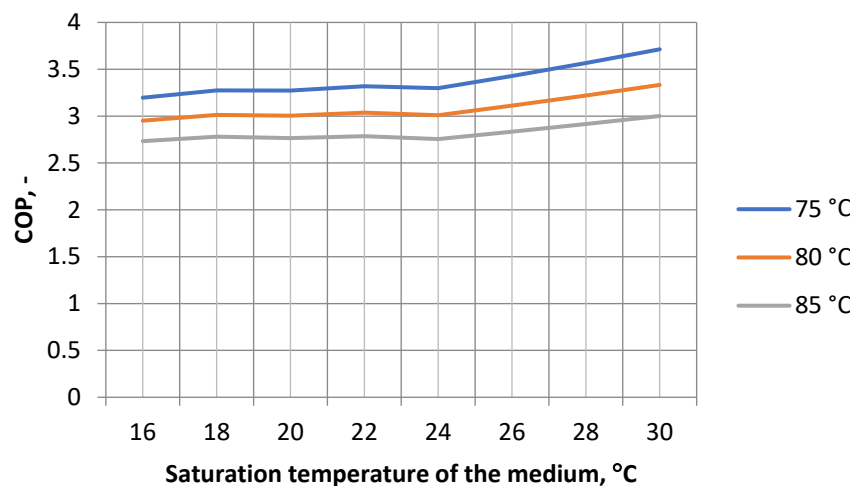


Figure 21. The COP value of the high-temperature heat pump with 100% control of both compressors for refrigerant condensing temperatures 75–85 °C.

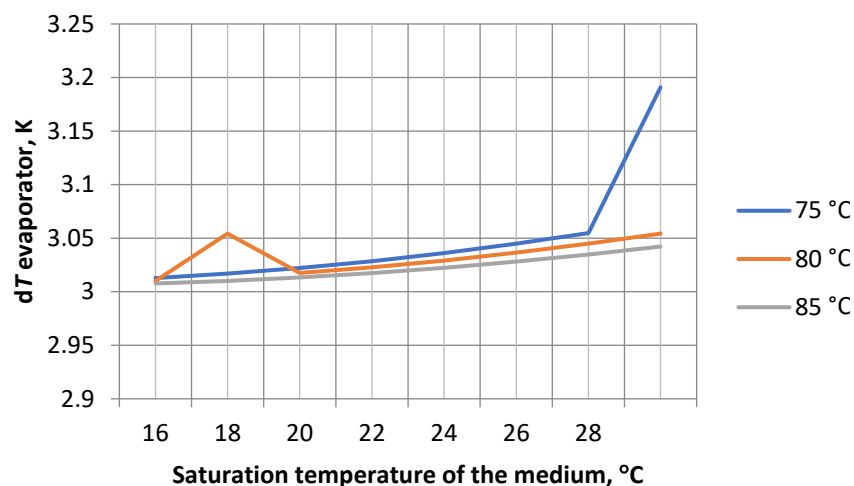


Figure 22. Quality of dT regulation of the working medium flowing through the evaporator of a high-temperature heat pump with 100% control of both compressors for refrigerant condensing temperatures 75–85 °C.

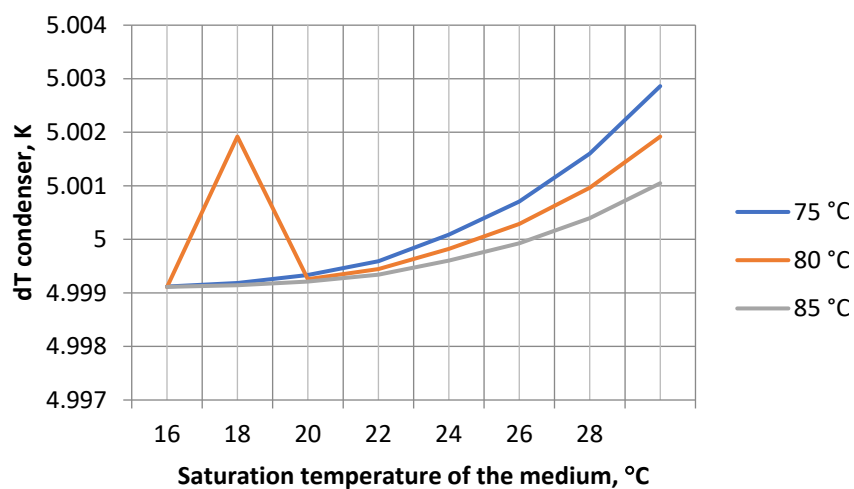
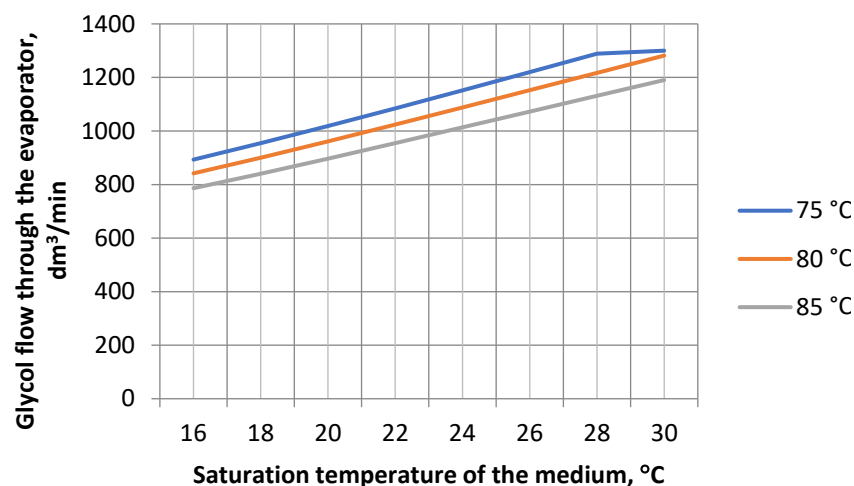
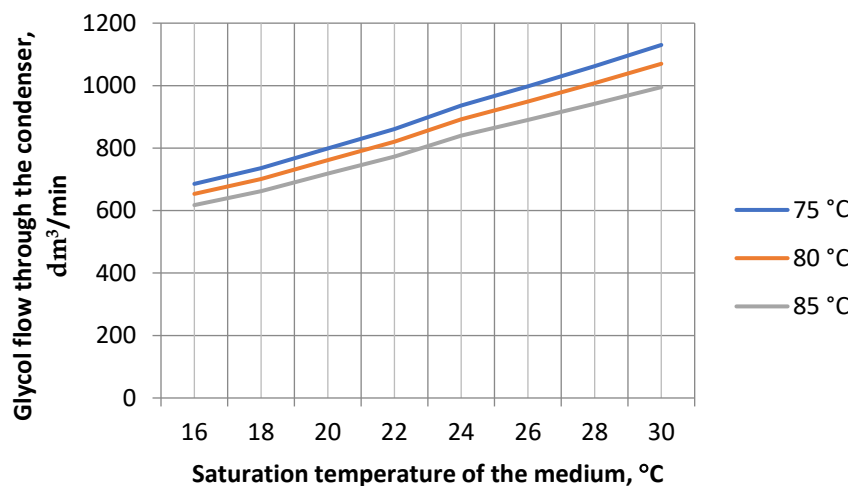


Figure 23. Quality of dT regulation of the working medium flowing through the condenser of a high-temperature heat pump with 100% control of both compressors for refrigerant condensing temperatures 75–85 °C.



**Figure 24.** Volume flow of the working medium through the evaporator of a high-temperature heat pump with 100% control of both compressors for refrigerant condensing temperatures 75–85 °C.



**Figure 25.** Volume flow of the working medium through the condenser of a high-temperature heat pump with 100% control of both compressors for refrigerant condensing temperatures 75–85 °C.

The dependence of heating power on the refrigerant's saturation temperature is presented similarly (Figure 19). The device generates the highest heating power value of 315.9 kW for the refrigerant's highest design saturation temperature (30 °C) and the lowest condensation temperature (75 °C). For this operating point, the power of both compressors is 85 kW. In the case of an increase in the condensation temperature from 75 °C to 85 °C at a constant saturation temperature of the refrigerant of 30 °C, the heating power received from the condenser will decrease from 315.9 kW to 282.9 kW, and the power of the compressors will increase to 94.2 kW. The lowest value of heating power is obtained for the saturation temperature of the refrigerant of 16 °C and its condensation temperature of 85 °C. The heating power value for this operating point is 188.1 kW with a compressor power demand of 59.8 kW.

A particular trend can be observed by analyzing the variation in the compressor power controlled at 100% as a function of the refrigerant saturation temperature. In the entire range of the refrigerant saturation temperature, the compressor power increases regardless of the upper source temperature, while in the saturation temperature range of 16–24 °C, it increases more steeply than in the saturation temperature graph of 24–30 °C (Figure 20).

As a result, the variation in the COP coefficient over the entire range of the refrigerant saturation temperature of the designed device for the design temperatures of the upper source is similar. The maximum value of the COP coefficient of 3.71 is achieved for the

refrigerant saturation temperature of 30 °C and the condensation temperature of 75 °C. The lowest value of the COP coefficient (2.78) occurs for the highest condensation temperature of 85 °C and the lowest saturation temperature of 16 °C (Figure 21).

Analyzing the quality of regulation obtained using the designed PI controllers, it is visible that in the case of the evaporator, the regulation deviation is maximally 0.19 °C, and the smallest is close to 0 (Figure 22). In the case of the condenser; the regulation deviation is at the level of  $\pm 0.003$  °C (Figure 23). The reason for the deviation of the parameters in Figures 22 and 23 results from the mass flow of the working medium. The temperature delta was not achieved exactly as 3.0 and 5.0 (3.05, 3.19 and 5.002, respectively).

The simulation studies allowed the calculation of the required flow of the working medium on the evaporator's primary and the condenser's secondary sides. For both the evaporator and the condenser, the required flow of the medium increases linearly for a constant saturation temperature of the refrigerant and an increase in the lower source temperature. In the case of the evaporator, the enormous volumetric flow is 1300 dm<sup>3</sup>/min (Figure 24). In the case of the condenser, the maximum flow value is 1130.1 dm<sup>3</sup>/min (Figure 25). The calculated values of the mass flow through the evaporator and condenser allowed the selection of circulation pumps forcing the flow of the working medium through the primary side of the evaporator and the secondary side of the condenser.

The piston compressors can regulate volumetric efficiency in 30–50 Hz. It allows the device's efficiency to meet the current demand for technological cooling.

#### 4. Conclusions

The article presents a project of an innovative line for the recovery of low-temperature technological heat generated during the production of stretch film using the cast method and its transformation into high-temperature heat. High-temperature heat is used to standardize the raw material of recycled origin. The share of recyclates can be up to 80%. The heat recovery line is based on two cascade-hydraulically coupled compressor heat pumps. The heat pumps are supplied with ecological refrigerants whose GWP coefficients are <150. The developed solution implements a closed-loop economy, is based on renewable energy sources, reduces energy consumption and CO<sub>2</sub> emissions and is in line with the European Green Deal. The technology developed is currently being implemented by the leader of the TW Plast consortium.

**Author Contributions:** Conceptualization, P.O. and J.S.; methodology, P.O. and J.S.; software, P.O. and K.G.; validation, P.O., J.S. and M.A.; formal analysis, P.O., K.G., M.A. and J.S.; data curation, P.O.; writing—original draft preparation, K.G. and P.O.; writing—review and editing, K.G. and P.O.; visualization, P.O., J.S. and M.A.; project administration, P.O. All authors have read and agreed to the published version of the manuscript.

**Funding:** This research was funded by the National Centre for Research and Development, Poland, grant number: POIR.01.01.01-00-1078/21.

**Data Availability Statement:** Data are contained within the article.

**Conflicts of Interest:** The authors declare no conflicts of interest.

#### References

1. Alsabri, A.; Tahir, F.; Al-Ghamdi, S.G. Environmental Impacts of Polypropylene (PP) Production and Prospects of Its Recycling in the GCC Region. *Mater. Today Proc.* **2022**, *56*, 2245–2251. [[CrossRef](#)]
2. Balu, R.; Dutta, N.K.; Roy Choudhury, N. Plastic Waste Upcycling: A Sustainable Solution for Waste Management, Product Development, and Circular Economy. *Polymers* **2022**, *14*, 4788. [[CrossRef](#)] [[PubMed](#)]
3. Chen, H.; Wan, K.; Zhang, Y.; Wang, Y. Waste to Wealth: Chemical Recycling and Chemical Upcycling of Waste Plastics for a Great Future. *ChemSusChem* **2021**, *14*, 4123–4136. [[CrossRef](#)]

4. Chen, X.; Chen, S.; Xu, Z.; Zhang, J.; Miao, M.; Zhang, D. Degradable and Recyclable Bio-Based Thermoset Epoxy Resins. *Green Chem.* **2020**, *22*, 4187–4198. [[CrossRef](#)]
5. Sarker, M.; Kabir, A.; Rashid, M.M.; Molla, M.; Din Mohammad, A.S.M. Waste Polyethylene Terephthalate (PETE-1) Conversion into Liquid Fuel. *J. Fundam. Renew. Energy Appl.* **2011**, *1*, 1–5. [[CrossRef](#)]
6. Thakur, M.; Sharma, A.; Chandel, M.; Pathania, D. Modern Applications and Current Status of Green Nanotechnology in Environmental Industry. In *Green Functionalized Nanomaterials for Environmental Applications*; Elsevier: Amsterdam, The Netherlands, 2022; pp. 259–281; ISBN 978-0-12-823137-1.
7. Wongsirichot, P. Natural Renewable Polymers Part I: Polysaccharides. In *Reference Module in Chemistry, Molecular Sciences and Chemical Engineering*; Elsevier: Amsterdam, The Netherlands, 2024; p. B9780443157424000077; ISBN 978-0-12-409547-2.
8. Singh, J.; Krasowski, A.; Singh, S.P. Life Cycle Inventory of HDPE Bottle-based Liquid Milk Packaging Systems. *Packag. Technol. Sci.* **2011**, *24*, 49–60. [[CrossRef](#)]
9. Hou, Q.; Zhen, M.; Qian, H.; Nie, Y.; Bai, X.; Xia, T.; Laiq Ur Rehman, M.; Li, Q.; Ju, M. Upcycling and Catalytic Degradation of Plastic Wastes. *Cell Rep. Phys. Sci.* **2021**, *2*, 100514. [[CrossRef](#)]
10. Ellis, L.D.; Rorrer, N.A.; Sullivan, K.P.; Otto, M.; McGeehan, J.E.; Román-Leshkov, Y.; Wierckx, N.; Beckham, G.T. Chemical and Biological Catalysis for Plastics Recycling and Upcycling. *Nat. Catal.* **2021**, *4*, 539–556. [[CrossRef](#)]
11. United Nations Framework Convention on Climate Change. Adoption of the Paris Agreement. In Proceedings of the Conference of the Parties Twenty-First Session, Paris, France, 30 November–11 December 2015. Available online: <https://unfccc.int/resource/docs/2015/cop21/eng/109r01.pdf> (accessed on 1 September 2024).
12. Kanai, T.; Cakmak, M.; Polymer Processing Society (Eds.) *Film Processing*; Progress in Polymer Processing; Hanser/Gardner: Cincinnati, OH, USA, 1999; ISBN 978-1-56990-252-3.
13. Thuy, V.T.T.; Hao, L.T.; Jeon, H.; Koo, J.M.; Park, J.; Lee, E.S.; Hwang, S.Y.; Choi, S.; Park, J.; Oh, D.X. Sustainable, Self-Cleaning, Transparent, and Moisture/Oxygen-Barrier Coating Films for Food Packaging. *Green Chem.* **2021**, *23*, 2658–2667. [[CrossRef](#)]
14. Kumar, J.C.R.; Majid, M.A. Renewable Energy for Sustainable Development in India: Current Status, Future Prospects, Challenges, Employment, and Investment Opportunities. *Energy Sustain. Soc.* **2020**, *10*, 2. [[CrossRef](#)]
15. Attanayake, K.; Wickramage, I.; Samarasinghe, U.; Ranmini, Y.; Ehalapitiya, S.; Jayathilaka, R.; Yapa, S. Renewable Energy as a Solution to Climate Change: Insights from a Comprehensive Study across Nations. *PLoS ONE* **2024**, *19*, e0299807. [[CrossRef](#)] [[PubMed](#)]
16. Ozyurt, O.; Ekin, D.A. Experimental Study of Vertical Ground-Source Heat Pump Performance Evaluation for Cold Climate in Turkey. *Appl. Energy* **2011**, *88*, 1257–1265. [[CrossRef](#)]
17. Spitler, J.; Gehlin, S. Measured Performance of a Mixed-Use Commercial-Building Ground Source Heat Pump System in Sweden. *Energies* **2019**, *12*, 2020. [[CrossRef](#)]
18. Correa-Quintana, E.; Muñoz-Maldonado, Y.; Ospino-Castro, A. Financial Evaluation of Alternatives for Industrial Methanol Production Using Renewable Energy with Heat Pump Technology. *Energies* **2024**, *17*, 5560. [[CrossRef](#)]
19. Chen, H.; Guo, S.; Song, X.; He, T. Design and Evaluation of a Municipal Solid Waste Incineration Power Plant Integrating with Absorption Heat Pump. *Energy* **2024**, *294*, 131007. [[CrossRef](#)]
20. Ghaderi, M.; Reddick, C.; Sorin, M. A Systematic Heat Recovery Approach for Designing Integrated Heating, Cooling, and Ventilation Systems for Greenhouses. *Energies* **2023**, *16*, 5493. [[CrossRef](#)]
21. Ma, D.; Sun, Y.; Ma, S.; Li, G.; Zhou, Z.; Ma, H. Study on the Working Medium of High Temperature Heat Pump Suitable for Industrial Waste Heat Recovery. *Appl. Therm. Eng.* **2024**, *236*, 121642. [[CrossRef](#)]
22. Calleja-Anta, D.; Nebot-Andres, L.; Cabello, R.; Sánchez, D.; Llopis, R. A3 and A2 Refrigerants: Border Determination and Hunt for A2 Low-GWP Blends. *Int. J. Refrig.* **2022**, *134*, 86–94. [[CrossRef](#)]
23. Ally, M.R.; Sharma, V.; Nawaz, K. Options for Low-Global-Warming-Potential and Natural Refrigerants Part I: Constrains of the Shape of the P–T and T–S Saturation Phase Boundaries. *Int. J. Refrig.* **2019**, *106*, 144–152. [[CrossRef](#)]
24. Nawaz, K.; Ally, M.R. Options for Low-Global-Warming-Potential and Natural Refrigerants Part 2: Performance of Refrigerants and Systemic Irreversibilities. *Int. J. Refrig.* **2019**, *106*, 213–224. [[CrossRef](#)]
25. Regulation (EU) 2024/573 of the European Parliament and of the Council of 7 February 2024 on Fluorinated Greenhouse Gases, Amending Directive (EU) 2019/1937 and Repealing Regulation (EU) No 517/2014. Available online: <http://data.europa.eu/eli/reg/2024/573/oj> (accessed on 2 May 2024).
26. IEC 60335-2-89; Household and Similar Electrical Appliances—Safety—Part 2-89: Particular Requirements for Commercial Refrigerating Appliances and Ice-Makers with an Incorporated or Remote Refrigerant Unit or Motor-Compressor. IEC: Geneva, Switzerland, 2019.
27. IEC 60335-2-40; Household and Similar Electrical Appliances—Safety—Part 2-40: Particular Requirements for Electrical Heat Pumps, Air-Conditioners and Dehumidifiers. IEC: Geneva, Switzerland, 2024.
28. Bitzer Software. Available online: <https://www.bitzer.de/websoftware/calculate/hhk/?tab=results> (accessed on 1 May 2024).

29. Dziadowiec, D.; Matykiewicz, D.; Szostak, M.; Andrzejewski, J. Overview of the Cast Polyolefin Film Extrusion Technology for Multi-Layer Packaging Applications. *Materials* **2023**, *16*, 1071. [[CrossRef](#)] [[PubMed](#)]
30. Obstawski, P.; Słoma, J.; Górnicki, K.; Awtoniuk, M. New Energy-Saving Technology for Industrial Stretch Foil Production. *Adv. Sci. Technol. Res. J.* **2025**, *19*, 271–282. [[CrossRef](#)] [[PubMed](#)]

**Disclaimer/Publisher’s Note:** The statements, opinions and data contained in all publications are solely those of the individual author(s) and contributor(s) and not of MDPI and/or the editor(s). MDPI and/or the editor(s) disclaim responsibility for any injury to people or property resulting from any ideas, methods, instructions or products referred to in the content.